

# ANALYSIS OF SURFACE NITRIDES CREATED DURING "DOPING" HEAT TREATMENTS OF NIOBIUM\*

J. K. Spradlin<sup>†</sup>, A. D. Palczewski, H. Tian, and C. E. Reece  
Jefferson Lab, Newport News, VA, USA

## Abstract

The benefits of reduced RF losses from interstitial "doping" of niobium are well established. Many of the details involved in the process remain yet to be elucidated. The niobium surface reacted with low-pressure nitrogen at 800°C presents a surface with chemical reactivity different than standard niobium. While standard "recipes" are being used to produce cavities, we seek additional insight into the chemical processes that may be used to remove the "undesirable" as-formed surface layer. This may lead to new processing routes or quality assurance methods to build confidence that all surface "nitrides" have been removed. We report a series of alternate chemistry treatments and subsequent morphological examinations and interpret the results. We also introduce a new standardized Nb sample system in use for efficient characterization of varying doping protocols and cross-laboratory calibration.

## INTRODUCTION

Improving the performance of SRF cavities becomes more difficult as the technology reaches the theoretical limits. Recent developments in SRF cavity processes leverages the diffusion of nitrogen into the Nb surface to improve the cryogenic RF performance. Understanding how the interstitial nitrogen improves the quality of the niobium is fundamental to developing a robust reliable process for SRF cavity preparation. Small samples of representative Nb coupons enable investigations of the nitration processes that are otherwise confounded or impractical with cavities. Witness samples facilitate analytical characterization of the surface morphology, chemical composition, and near surface crystallinity for representative nitration processes without sacrificing a cavity. Investigations of various nitration processes and post nitration chemistry effects have correlated SEM observations and EBSD data to suggest explanations for nitration cavity inconsistencies in RF performance.

## NITRATION PROCESSES

Improving niobium SRF performance with nitrogen interstitials was first reported by A. Grassellino in 2013 [1]. It was shown that N<sub>2</sub> exposure to niobium lacking a passivating oxide during thermal treatments improved SRF performance to a new standard. The performance benefit of 2-3 improvement in Q<sub>0</sub> and field enhancement are only realized after chemical removal of some thickness. The RF response as a function of doping protocol and removal

thickness is not yet well characterized. Benefits in RF performance are only realized in Nb that has been uniformly polluted with nitrogen and is completely absent of Nb<sub>2</sub>N phases. Nitrogen is reported as the most significant Columbic scattering center for all elemental impurities considered in Nb sheet specifications with dislocation densities around 10<sup>8</sup> cm<sup>-3</sup> in recrystallized material [2]. First-principles calculations of nitrogen energetics in a niobium lattice indicate that nitrogen blocks hydrogen residence in the lattice by preferentially occupying vacancies and octahedral interstitial sites [3] and nitrogen is a more energetically favorable interstitial impurity than oxygen or carbon [4]. Calculations from lattice modeling support the observations that nitrogen spontaneously diffuses into niobium up to some critical concentration and nitrogen interstitials reduce lattice availability for hydrogen [3, 4, 5]. After the nitration process, the niobium surface is polluted with crystallites that increase RF losses [1, 6]. Studies by Trenikhina et al. named the crystallite phase as Nb<sub>2</sub>N and identified local crystallographic relationships to niobium [6]. The specific conditions that precipitate Nb<sub>2</sub>N phases in the niobium surface has not been reported. The effective diffusion rates, critical concentration of nitrogen (lattice saturation), density distribution profile, and chemical properties have not been specifically reported for SRF niobium nitration processes.

## SAMPLE PREPARATION

A set of samples was created to provide a well-controlled base material to characterize the effects of different nitration processes. While other characterization tools are useful, as previously demonstrated, the chief tool for analysis of the interstitial content of surface niobium is secondary ion mass spectrometry (SIMS). While SIMS can be very sensitive to low concentration components, obtaining calibrated quantitative results is non-trivial and time-consuming [7]. We thus tailored our sample format to best integrate with SIMS analysis.

We established a collaborative relationship with the Nanoscale Characterization and Fabrication Lab (NCFL) at Virginia Tech (VT) to engage the use of their Cameca IMS 7f GEO dynamic SIMS in our investigations. In order to be time and cost effective in the use of the instrument, we settled on 6 × 10 mm sections cut from standard RRR grade 2.8 mm SRF cavity cell sheet stock. This sample format accommodates 5 samples plus one implant standard on each stage loaded for SIM's analysis.

Tokyo Denkai niobium sheets purchased under the LCLS-II specification were first heat treated to 900 °C for 3 hour in a vacuum oven at ~ 1×10<sup>-6</sup> Torr [8]. The sheets were then cut by wire electro-discharge machining to size and BCP etched a nominal amount of 50 μm. The coupons

\* Work supported by U.S. DOE Contract No. DE-AC05-06OR23177 with funding support from the Office of Nuclear Physics and LCLS-II-HE Project.

<sup>†</sup> spradlin@jlab.org

were then nanopolished on one major face by Surface Finishes (Addison II USA) to a flatness of 200–300 nm. While the nanopolish yielded planar surfaces quite suitable for depth profiling with SIMS, we found that there was occasional residual polishing media imbedded in the surface. Additionally, the coupons were suspected of having a surface crystallinity that was not representative of a cavity. To correct the disparity in surface quality of the coupons, the nanopolished coupon faces were electropolished in a 10:1 mixture of  $H_2SO_4$  (98%):HF(49%) at room temperature in a potentiostatic cell using an aluminum cathode with ~10 V applied cell potential (~10 cm working distance) for a total removal of at least 10  $\mu m$ . Electropolishing the coupons maintained the nanopolished flatness and improved the crystallinity.

## SAMPLE USE

The niobium coupons were used as witnesses, processed together with niobium cavities during furnace heat treatment runs. In order to build confidence in the uniformity of process conditions in various furnaces, samples have been included in furnace runs at DESY, FNAL, Cornell University, Research Instruments GmbH, Ettore Zanon SpA, and also supplied to KEK. The intent is to have standardized samples and standardized analysis so that unrecognized process differences might be uncovered and underlying process dependencies elucidated. It remains yet to be demonstrated that the various furnaces and process controls are functionally equivalent to a detailed level.

The normal routine with “doped” small samples is to perform a brief SEM morphological examination, then give each sample surface a 5  $\mu m$  EP analogous to a typical “doped” cavity EP, re-inspect with SEM, and then route them for SIMS concentration depth profile characterization for elements N, O, and C to a typical depth of 1.5  $\mu m$ , occasionally 8  $\mu m$ . Results to date from the SIMS measurements are contributed to this conference in A. Palczewski and J. Angle contributions [9, 10].

## CHARACTERIZATION WITH SEM

After completion of the nitration furnace run the samples were investigated with a Tescan VEGA 3 XMH LaB<sub>6</sub> scanning electron microscope (SEM) equipped with EDAX EDS and EBSD detectors. Inspecting samples before SIMS measurements with the SEM allows screening of the samples and provides a correlation of the observed topography with the depth profile data.

### Expected Surfaces after 5 $\mu m$ EP

A set of 4 samples treated together with cavities at Research Instruments (RI) were examined by SEM with incremental EP removals. Three process states are presented in Fig. 1. Each column of images corresponds to a specific sample processed by RI and the top row of images represents the as-nitrided surfaces, the middle row corresponds

to the 1  $\mu m$  EP surfaces, and bottom row presents 5  $\mu m$  EP images. In the top row, each image presents a single “doped” grain for each sample. Two different doping protocols are represented, 3N60 and 2N0. Incremental EP cycles were conducted to visualize the Nb<sub>2</sub>N distribution and orientation in the Nb surface. It was observed, however, that in short < 1  $\mu m$ , EP cycles, the observed Nb surface had pits ~1–1.5  $\mu m$  deep with densities similar to the observed pyramidal densities of the as-nitrided samples. Despite significant differences in the 1  $\mu m$  EP surfaces, all of the samples look similar at a 5  $\mu m$  EP depth. The images of the 5  $\mu m$  EP are indicative of ideal cavity surfaces.

### Unexpected Surfaces after 5 $\mu m$ EP

For some nitration samples, representative of a cavity ready for RF testing (a “doped” Nb surface with 5  $\mu m$  EP), upon SEM inspection we observed instances suggesting that Nb<sub>2</sub>N phases had formed at some depth below the surface.

On at least two samples each subjected to 2N0 and 3N60 protocols and controlled 5  $\mu m$  EP, specific localized grains were found to have a surface somewhat recessed with respect to the mean plane and also decorated with pyramidal topography quite similar to but about 1/10 scale to that observed on the surface of “as-doped” niobium. See Fig. 2. Further characterization is needed, but this has the appearance of a deeper set of nitrides than has not been previously recognized. Specific Nb properties that may cause pyramid formation 4–5  $\mu m$  below the surface have not been previously considered.

In a few cases, there have been grains observed in the as-nitrided surface that have no pyramids while surrounding grains have expected densities. One may speculate that there are some thin, or shallow, grains with too little volume or capacity to support precipitation of the Nb<sub>2</sub>N phase. It may also be that at particular grain boundary angles assisted diffusion leads to locally higher conductances of N interstitials that saturate at some properly oriented subsurface grain.

The potential implications of such a finding are important. If there are specific combinations of “unlucky” grain orientations and thicknesses that promote significantly deeper nitride formation in “N-doped” niobium, this might be an explanation for variability of cavity quench field levels with all other factors constant. Further investigation is quite warranted.

### Unexpected Surfaces after HF Soak

After inspecting the initial nitration surface, some small samples were subjected to atypical chemical etches in an effort to find an etchant that could selectively remove the nitride phases. It is well accepted that concentrated HF at room temperature does not significantly etch pure Nb. Sulfuric acid in any concentration at room temperature does not have an adequate chemical potential to etch Nb.

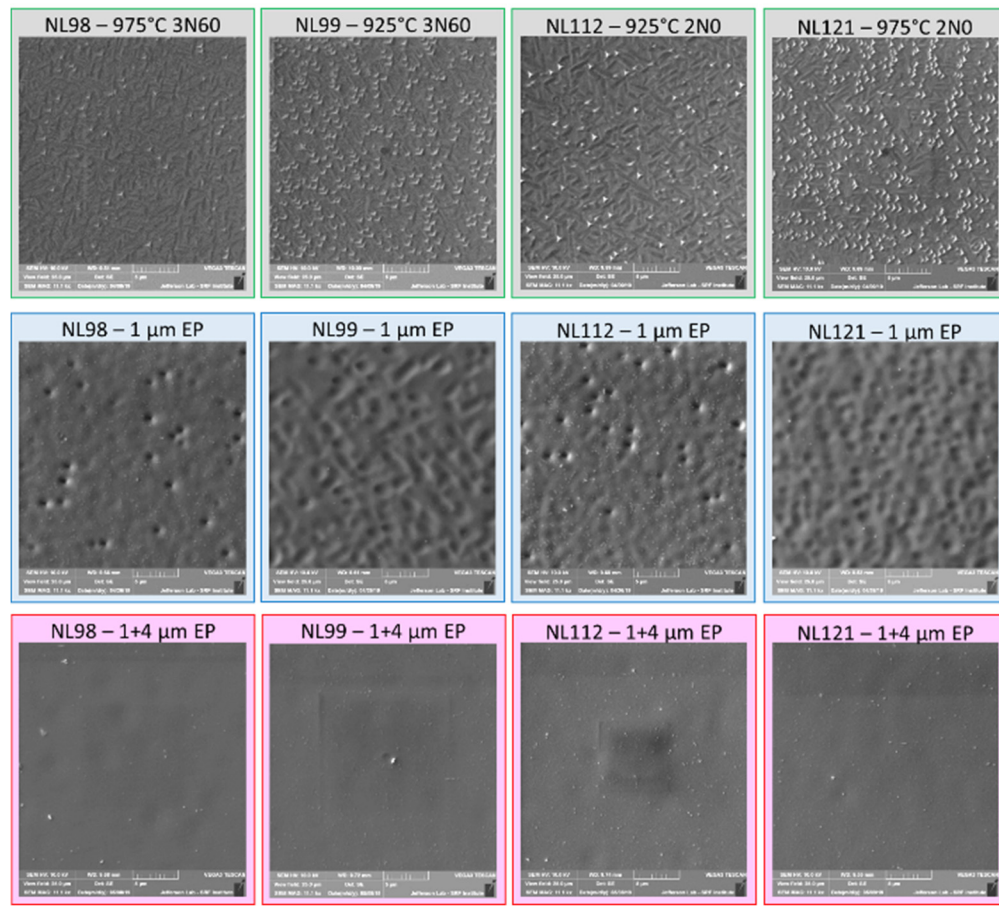


Figure 1: Images for (4) vendor-treated samples with different nitration recipes (top row). 1  $\mu\text{m}$  EP (middle row), and 5  $\mu\text{m}$  EP (bottom row). All SE images are 25 $\times$ 25  $\mu\text{m}$  scale.

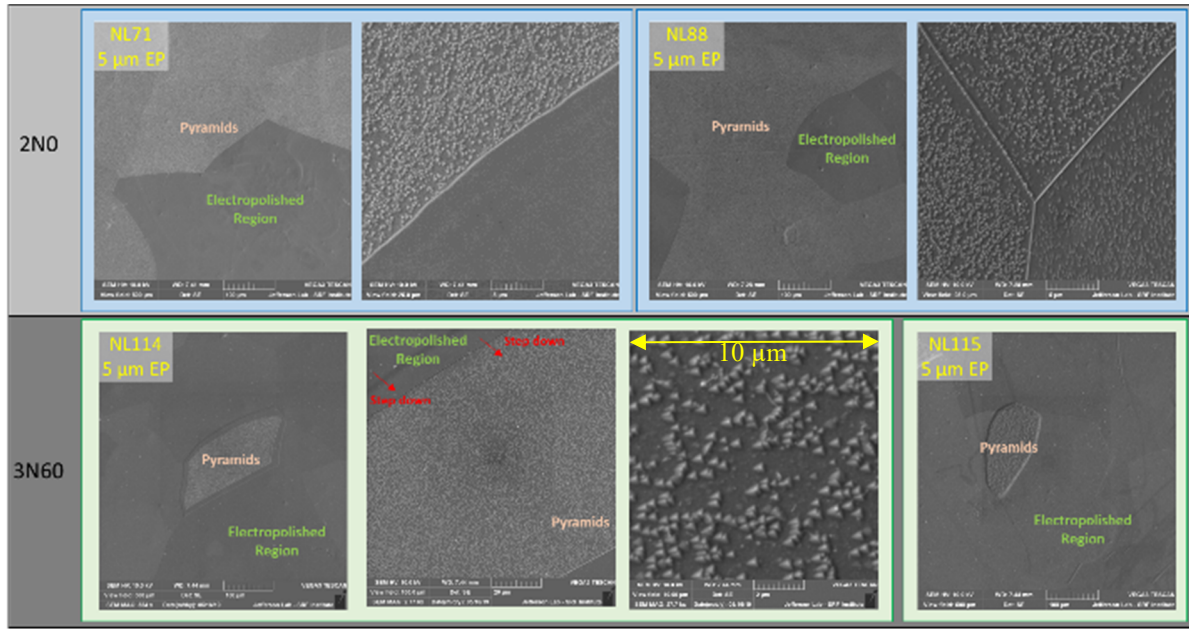


Figure 2: Images of doped Nb coupons' final EP surface.

A series of investigations were pursued to determine the reactivity of  $\text{Nb}_2\text{N}$  in HF and  $\text{H}_2\text{SO}_4$  at room temperature. A comparison of the process states for NL115, a 3N60 sample produced in the Elnik vacuum furnace inside a single cell cavity with high conductance cavity caps at JLab, is

presented as Fig. 3. The images on the left are representative of as-nitrided 3N60 surface.

The effects of exposure to HF alone was surprising. Conventional experience is that HF dissolves any  $\text{Nb}_2\text{O}_5$ , but leaves bulk Nb unaffected. (Thus the use of "HF rinses" to

remove only a few nm per cycle.) A 1 hour soak in concentrated HF selectively chemically etched  $\sim 0.5 \mu\text{m}$  of the Nb surface excavating the  $\text{Nb}_2\text{N}$  precipitates. Highly disturbed niobium near the surface of a “nitrided” sample was removed, leaving behind apparently intact, but slightly modified  $\text{Nb}_2\text{N}$  crystals. The sample was subjected to an additional 6 hours of HF where it was determined that the etchant had exhausted activity. It was determined by SEM examination that the etchant was anisotropic, removing a grain dependent thickness and producing a grain specific roughness of the surface. The roughness suggests that there is grain orientation dependency of nitride diffusion depth within the first micron, potentially also the absorbed concentration, and consequently the resulting effective chemical potential probed in the HF removal. The sample showed no change after a 6 hr soak in concentrated  $\text{H}_2\text{SO}_4$  at room temperature.

Comparing the upper and lower images across the panels in Fig. 3 demonstrates the varying density of nitride pyramidal features on different grains of the niobium. The center two images are representative of the surface observed after a 1 hour concentrated HF soak at room temperature. The pyramidal features are evolving in area and height from the surrounding defective Nb etch plane.

Comparing the density in the top and bottom center images demonstrates again the grain orientation dependency of the pyramid density and the pyramid characteristic length scales (physical size and diffusion/inhibition zones). The bottom center image represents extremes in pyramid feature disparity, the larger featured lower density, precipitates are visible on the left and the smaller featured higher density nitrides are evident on the right. The right two images are representative of the observed surface after

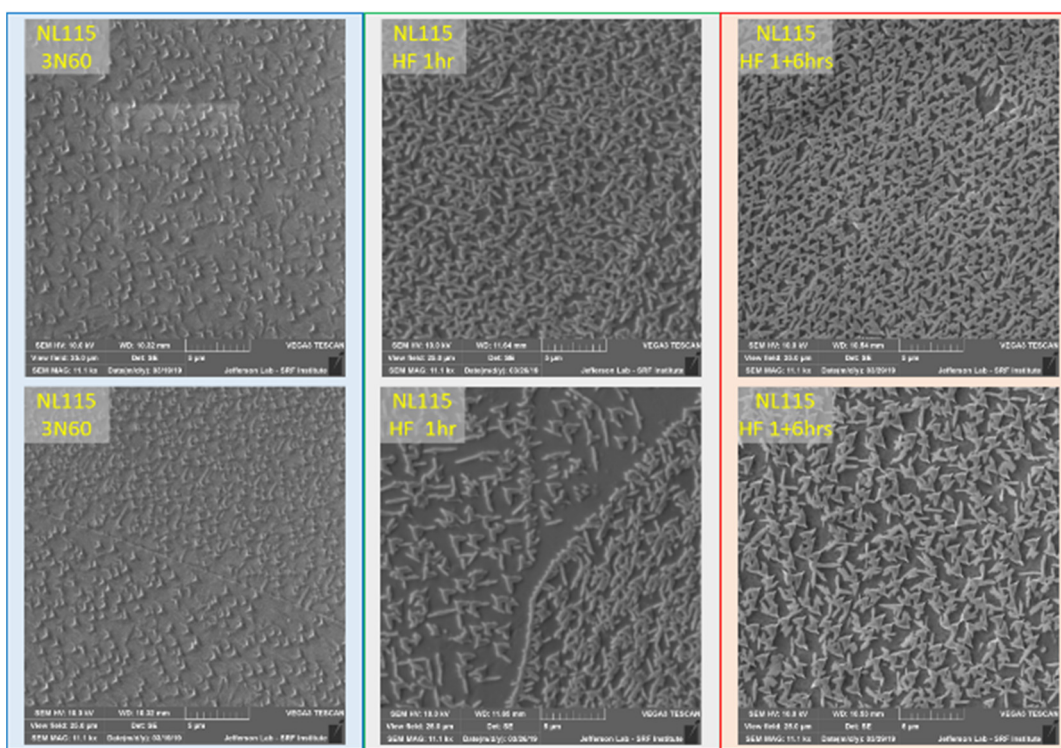


Figure 3: Comparison of Niobium surface for 3N60 sample after nitration (left images), nitration + 1 hour HF soak (center images), and 1 + 6 hours HF soak (right images). All SE images are  $25 \times 25 \mu\text{m}$  scale.

the additional 6 hour HF soak. Comparing the 1+6 hr HF soak to the 1 hr HF soak indicates further etching and complete excavation of the  $\text{Nb}_2\text{N}$ . In all process states the densities, characteristic orientations, and size of the observed features varied with Nb grain.

Further analysis of the bottom image offers some new insight into the nitration precipitation physics. The  $\text{Nb}_2\text{N}$  features observed are in two distinct orientations which appear approximately orthogonal. Several other structures are observed other than pyramids. It is likely that the geometry of the nitrides would be context sensitive, i.e. structurally influenced. The total feature density was around mid  $10^8$  features per  $\text{cm}^2$ .

It is unclear whether the feature orientations in the HF soak images are representative of the pyramidal positions before the HF soak. It seems unlikely that the features settled or rotated significantly during the removal of the surrounding defective Nb. The features have 2 or 3 preferred orientations at characteristics angles of  $\sim 90^\circ$  and  $\sim 60^\circ$  in any of the 1 hr or 1+6hr fields of view. The uniformity of arrangement is statistically inconsistent with randomized rotations or settling. The precipitates appear to have anchor points on the Nb surface that are strong enough to resist generalized forces such as water rinsing and anti-static nitrogen but were not adhered to the surface sufficiently to withstand direct mechanical abrasion.

A region of the HF-soaked sample was selected for EBSD analysis, Fig. 4, where several neighboring grains had been mostly swept free of surface nitride crystals. The region selected had five grains visible in the SE image from differential HF etching. In Fig. 4, the left panel is the SE image with grains labeled and the EBSD region identified by the red rectangle. The middle panel is the EBSD inverse pole figure of the selected region. On the right, there is a representative Kikuchi pattern for each Nb grain orientation with a ranking for the degree of grain etching and the estimated pyramidal density extrapolated from morphological and tilted SE imaging.

Serendipitously, the areas swept mostly free of precipitates provided a unique perspective on the relationship between the nitride features and the surrounding Nb. Grains 3 & 5 had the most etching, estimated at most to be  $2 \mu\text{m}$  of defective Nb, followed by grain 1, then grain 2, and the flattest grain with the least volume of Nb removed was grain 4. It is estimated that the thickness of defective Nb removed from regions like grain 4 was at most  $1.5 \mu\text{m}$ , likely closer to  $0.75 \mu\text{m}$  or less. Most of grain 4 still had  $\text{Nb}_2\text{N}$  pyramidal features present preventing the EBSD software from indexing the underlying bulk Nb orientation. Investigating grain 4 manually, it was found that the Kikuchi patterns obtained were likely a hexagonal phase consistent with Trenikhina et al. TEM data [6].

There is a strong correlation between the character of the Nb plane revealed by chemical etching and the  $\text{Nb}_2\text{N}$  features present. Grains with the least amount of Nb removed had higher densities of pyramidal features sitting on a shallow smooth Nb plane, while grains with the most Nb removed had larger  $\text{Nb}_2\text{N}$  pyramidal features sitting on rougher Nb grains with triangular terrace facetting. From the HF-soaked morphological observations presented in Fig. 3, there is an inversely proportional relationship between the  $\text{Nb}_2\text{N}$  density and size. Densely populated grains

had the smallest  $\text{Nb}_2\text{N}$  pyramids and the least thickness of Nb removed by HF alone.

## CONCLUSIONS

Careful preparation of reference samples and controlled studies parallelled with niobium SRF cavity work offers opportunities to better understand the material reality that yields the corresponding cavity performance. Rather straightforward use of an SEM for incremental process characterization and analysis has revealed unexpected reactivities and surfaces.

The precipitation of  $\text{Nb}_2\text{N}$  is observed to be quite variable with niobium grain orientation, at least within the first few microns. It is suspected that the precipitation variance is resulting from grain specific accumulation and transport of nitrogen into the niobium surface. Controlled EP on controlled samples reveals a grain-specific structure resulting from grain-specific N dynamics.

A method for using concentrated HF to selectively etch defective Nb to expose sub-surface nitration precipitates in “doped” Nb was used to aid in the process development for Nb “doping” recipes. Current data suggest that developing a robust process for SRF cavity production utilizing nitrogen interstitials is challenged by Nb material properties and nitrogen precipitate behavior.

Understanding the local conditions that lead to  $\text{Nb}_2\text{N}$  precipitation could be instrumental in nitration process development for SRF cavities. Studies are underway to determine the effects of nitration process parameters and Nb material properties on the formation of  $\text{Nb}_2\text{N}$  precipitates. Avoiding the presence of such precipitates in functional SRF surfaces is likely critical to realizing the full performance benefits of Nb “doping”.

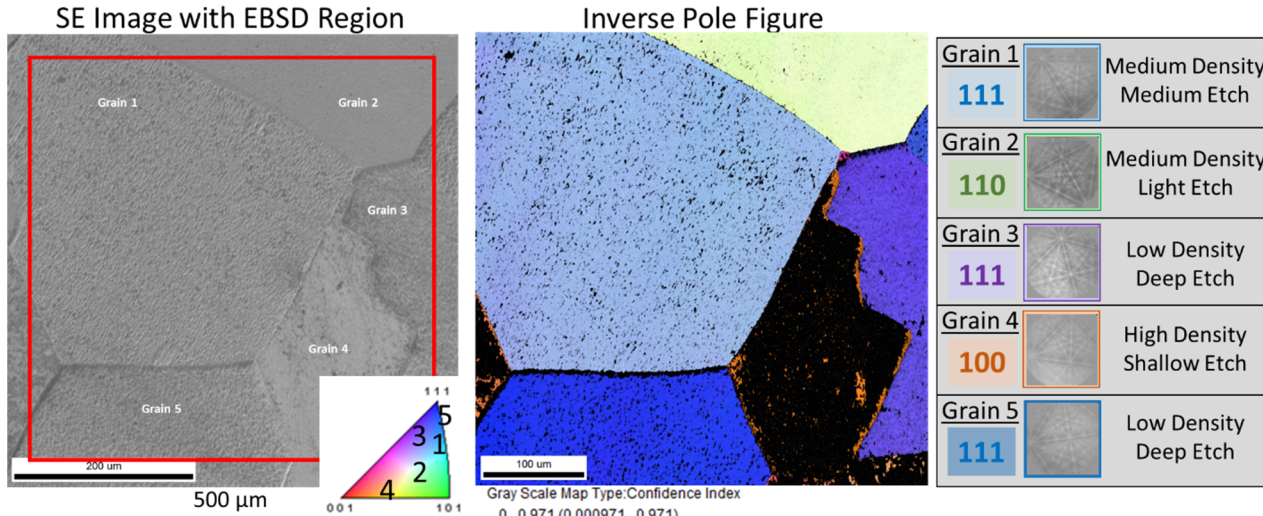


Figure 4: NL115 3N60 1 + 6 hour HF soak SEM and EBSD map of an abraded region.

## REFERENCES

- [1] A. Grassellino, et al., *Supercond. Sci. Tech.* 102001 (2013).
- [2] T. Carneiro, C. Klinkenberg, M. Imagumbai, Co. Ltd, and H. R. S. Moura, “High RRR Niobium Cost Reduction Program for SRF Linacs”, in *Proc. 10th Workshop RF Superconductivity* (SRF'01), Tsukuba, Japan, Sep. 2001, paper PR018, pp. 417-418.
- [3] P. Garg, I. Adlakha, K. N. Solanki, S. Balachandran, P. J. Lee, and T. R. Bieler, “Role of Nitrogen on Hydride Nucleation in Pure Niobium by First Principles Calculations”, in *Proc. 18th Int. Conf. RF Superconductivity* (SRF'17), Lanzhou, China, Jul. 2017, pp. 741-745. doi:10.18429/JACoW-SRF2017-THPB002
- [4] D. C. Ford, P. Zapol, & L. D. Cooley, *J. Phys. Chem. C* 14728 (2015).
- [5] D. C. Ford, L. D. Cooley, and D. N. Seidman, *Supercond. Sci. Technol.* 095002 (2013).
- [6] Y. Trenikhina, A. Grassellino, O. S. Melnychuk, and A. Romanenko, “Characterization of Nitrogen Doping Recipes for the Nb SRF Cavities”, in *Proc. 17th Int. Conf. RF Superconductivity* (SRF'15), Whistler, Canada, Sep. 2015, paper MOPB055, pp. 223-227.
- [7] J. Tuggle, et al., *J. Vac. Sci. & Technol. B* 052907 (2018).
- [8] W. Singer et al.. *Technical Specifications Niobium Material - 2016*. DESY, Hamburg, XFEL/007, Revision C May 07, 2010. Proceedings of IPAC, Busan, Korea WEPMB034
- [9] A. D. Palczewski, C. E. Reece, J. K. Spradlin, and J. W. Angle, “Development of a Qualitative Model for N-Doping Effects on Nb SRF Cavities”, presented at the 19th Int. Conf. RF Superconductivity (SRF'19), Dresden, Germany, Jun.-Jul. 2019, paper TUFUA3.
- [10] J. W. Angle, J. Tuggle, G. V. Eremeev, C. E. Reece, M. J. Kelley, and U. Pudasaini, “Crystallographic Characterization of Nb<sub>3</sub>Sn coatings and N-Doped niobium via EBSD and SIMS”, presented at the 19th Int. Conf. RF Superconductivity (SRF'19), Dresden, Germany, Jun.-Jul. 2019, paper THP017.